Top Catal (2010) 53:365–377
DOI 10.1007/s11244-010-9446-3

ORIGINAL PAPER

# Insights from Theory on the Relationship Between Surface Reactivity and Gold Atom Release

**Thomas A. Baker · Efthimios Kaxiras · Cynthia M. Friend**

Published online: 2 April 2010


**Abstract** Density functional theory, informed by experimental studies, is used to investigate the interplay of surface morphology, the adsorption site of reactants, the nature of the interaction between adsorbates and the surface, the potential energy landscape for adsorbates on the surface, adsorbate coverage, temperature, and the dynamic evolution of these factors during adsorption and reaction. We summarize our current understanding of Au atom release on the (111) surface and the corresponding effects on adsorption and reactivity. Gold was selected for these investigations because of the recent intense interest in the activity of gold nanoparticles for several important catalytic reactions. Fundamental experimental studies on Au single-crystal surfaces have established that atomic O is extremely active for oxidation of CO and olefins, that the local bonding of O is an important factor in determining the reactivity and selectivity for oxidation, and that Au atom release is induced by electronegative adsorbates, such as O, Cl, and S. These experimental results guided our theoretical studies. Density functional theory is an extremely useful tool since it evaluates the energetics associated with the incorporation of gold into the adsorbate layer, while providing fundamental physical insight into the underlying cause of gold incorporation. We use our results from static DFT calculations along with ab initio molecular dynamics simulations to understand the effect of surface morphology on the activity of gold for CO oxidation. Our investigation of Au atom release and incorporation induced by electronegative atoms clearly illustrates the importance of using experiments in combination with theory to establish the importance of and the underlying reasons for metal atom release and the affect on bonding and reactivity.

**Keywords** Density functional theory · Gold · Surfaces · Oxygen · Chlorine · CO oxidation · Atom release · Reactivity

T. A. Baker · E. Kaxiras · C. M. Friend (✉)
Department of Chemistry and Chemical Biology, Harvard University, 12 Oxford Street, Cambridge, MA 02138, USA
e-mail: friend@chemistry.harvard.edu

E. Kaxiras · C. M. Friend
School of Engineering and Applied Sciences, Harvard University, Cambridge, MA 02138, USA

E. Kaxiras
Department of Physics, Harvard University, 12 Oxford Street, Cambridge, MA 02138, USA

## 1 Introduction

Development of structure–reactivity relationships is a cornerstone in developing predictive models for chemical behavior in all fields of chemistry. In surface chemistry and catalysis, the types of coordination sites are widely recognized to be an important factor because their nature determines the local bonding of adsorbed species on surfaces, ammonia synthesis [1–3] being an established example. While well-defined surfaces can be prepared from single-crystal surfaces, the surface structure is not always an extension of the bulk and often changes when adsorbed species are present on the surface [4, 5], which is of deep fundamental importance to many areas of surface chemistry, especially catalysis and surface reactivity [6–9]. For example, adsorption on most fcc and hcp close packed metal surfaces will result in some reconstruction, buckling, or distortion of at least the first layer of metal atoms [10, 11]. Adsorbate induced restructuring of the (111) crystal faces of platinum and rhodium are important for C–H bond

activation [12, 13]. Oxygen-induced reconstructions are driven on many surfaces, including (but not limited to) Pt(111) [14, 15], Pt(110) [16, 17], Pd(111) [18], Ni(110) [19, 20], Cu(110) [21], Cu(111) [22], Fe(211) [23].

Dramatic changes in surface structure that include metal atom release from metal surfaces induced by adsorbed species has been established, even for close-packed surfaces [24]. Understanding metal atom release is crucial for a fundamental understanding of the surface chemistry of metals relevant to catalytic processes since the local bonding sites available, the overall surface morphology, and the ability of reactants to diffuse on the surface are all affected by metal atom release [4]. There are many examples of metal atom release. Tao et al. used experimental and theoretical tools to show that CO adsorption on hex-Pt(100) induces release of Pt, yielding metal nanoclusters on the surface [25]. Metal release and restructuring also occurs on Pt(100) with NO [26] and $O_2$ [27]. McCrea et al. found that formation of a platinum carbonyl species on Pt surfaces could drive metal atom release [28]. Dynamic restructuring of the Ag(111) surface occurs during the reaction of sulfur dioxide with Ag(111)-p(4 × 4)-O resulting in the incorporation of added silver atoms [29]. While a complete review is not within the scope of this report, it is evident that atom release from metal surfaces is a general phenomenon.

Controlling the morphology and reactivity of gold surfaces is particularly important because these surfaces play a vital role in all aspects of modern technology and science, from heterogeneous catalysis [30–33] to nanotechnology [34]. Supported gold nanoparticles can catalyze a wide variety of reactions including the reduction of $NO_x$ by hydrocarbons [35, 36], the oxidation $CH_4$ [37, 38], CO [39], and propene [40], and the epoxidation of propylene [41]. Gold is extensively used as a substrate for self-assembled monolayers (SAM) [42, 43] in materials science [44], as interconnects in electronic devices [45–47], as a substrate for conducting polymers in chemical sensors [48], and in many different types of biosensors [49, 50]. Gold can be used in plasmonic electronic devices and is an important substrate for surface enhanced Raman spectroscopy [51, 52]. Surface morphology, the local bonding, and the mobility of gold atoms are important in all of these applications, rendering it essential that the underlying basis for adsorbate-driven metal atom release be understood.

While gold incorporation may be one of the most important factors affecting the reactivity of gold surfaces, there are several other factors that control the catalytic activity of gold nanoparticles on oxide supports, although as we will explore, many are closely related to metal atom release. For example, the size [53, 54] and shape [55] of supported Au nanoparticles has a substantial effect on its catalytic activity [56]. Other factors that have been discussed in determining catalytic activity of Au-based materials include the nature of the metal oxide support, the oxidation state of Au, and the method by which the catalyst was prepared [57]. Recent results indicate that gold can be activated even in the absence of a reducible metal oxide support and that even large, micron-size gold particles are catalytically active. For example, micron-size gold powder is active for CO oxidation [58–60] and CO oxidative amination [57], and nanoporous Au promotes CO oxidation [59] and selective oxidation of glucose [61].

Experimentally, O bound to single-crystal gold is exceedingly active for a variety of oxidation reactions, whereas clean Au is essentially inert for these processes [62–64]. Molecular $O_2$ species may also promote some reactions, e.g. CO oxidation; however, analogy with Ag [65] suggests that adsorbed O, which behaves as a Brønsted base, is a key component of a broader range of oxidation reactions. Furthermore, the morphology of gold surfaces and particles is affected by O adsorption, based on experimental imaging studies [65, 66]. The local bonding of O, which depends on surface morphology, also affects activity for CO oxidation [62] and both the activity and selectivity for propene oxidation [67]. These results suggest that dynamic restructuring can occur during reaction, which will affect reaction kinetics as was recently illustrated for the reduction of resazurine on Au nanoparticles [68].

While the mechanism for oxidation on gold is still a controversial topic, it has been suggested that under-coordinated Au atoms are important for gold's activity [69–71] and could be possible sites for the binding and dissociation of $O_2$, an important step in the catalytic process [72–74]. Moreover, adsorption of CO and O is stronger on Au sites with lower coordination number [56]. It is, therefore, important to understand how under-coordinated atoms can be created on the surface and under what conditions they are stable. Gold atom release induced by adsorbed species is also important for understanding how agglomeration (sintering) of Au particles supported on metal oxide supports occurs, which is one mechanism for catalyst deactivation [75].

Theory in conjunction with fundamental studies of surface reactivity can provide guiding principles for understanding the catalytic properties of metals and can therefore be used for the future design of novel catalysts [76–78]. Advances in modern density functional theory (DFT) and the increase in computational power over the past decades have made relatively accurate, slab calculations feasible for systems important in catalysis. Norskov and coworkers have pioneered the use of DFT to successfully describe trends in reactivity for many transition metals and alloys [79–82]. For example, Norskov and others have illustrated how simple bond strength correlations can be used as a guide for establishing metals that are best for particular

reactions [83, 84]. Linear relationships exist between dissociation activation energies and enthalpy changes, known as Brønsted–Evans–Polanyi (BEP) relationships, which have been very useful for describing the activity of transition metals [85, 86]. Electronic considerations are also important for understanding adsorption and reactivity. Norskov and coworkers have found a coupling between the adsorbate valence states and the transition metal d-states; the higher the energy of d-states relative to the Fermi energy of the metal, the stronger the interaction of the adsorbate [87, 88]. DFT calculations have also been used to show that low coordination sites on metal surfaces are important. Along with the examples important for gold oxidation [56, 72, 89, 90] it was found that steps were important in calculating the rate of ammonia synthesis on ruthenium nanoparticle catalysis [91], for methane activation on Ni [92, 93], and for carbon monoxide oxidation on Ru(0001) [94] and other metal surfaces [95]. It is important to point out that experimental surface science studies provide critical information for constructing and testing theoretical models, such as unit cell dimension, surface morphology, and vibrational frequencies.

Herein, we review recent work from our groups aimed at understanding the interplay between adsorbate bonding and surface morphology of flat and defective Au(111) using state-of-the-art DFT calculations and comparison to experimental measurements. In the first section we investigate how the adsorption of electronegative atoms (specifically oxygen, chlorine, and sulfur) on Au(111) will incorporate gold atoms into the adsorbate layer. We understand how the coverage can affect this incorporation and try to provide physical insight into the cause of this incorporation. In the second section, we review how DFT and ab initio molecular dynamics (AIMD) was used to understand how the morphology of the surface and gold incorporation into the adsorbate layer can affect the bonding of O and the activity for CO oxidation. Finally, we place our work in a broader context and outline remaining challenges in understanding reactivity relevant to heterogeneous catalysis.

## 2 Computational Methods

A variety of theoretical tools are used throughout this report, with the exact details described elsewhere [96–99]. To summarize, static calculations and AIMD simulations were performed in the framework of density functional theory using the VASP code [100] often with the GGA-PW91 functional and ultrasoft pseudopotentials [101–103]. Other functionals were tested and used in cases where the GGA-PW91 functional was not appropriate. In each case the plane-wave cutoff energy, k-space sampling, supercell size and number of layers, electronic and ionic convergence tolerance, and other parameters were tested over a range of values and converged to provide accurate results. AIMD calculations were performed in the canonical ensemble [104], with a time step of 2 fs, for the reaction of carbon monoxide with atomic oxygen covered Au(111). At each oxygen coverage, 100 independent simulations were performed, each lasting 8 ps. All results are obtained after a sufficient equilibration time, as evaluated by the point in time at which fluctuations in the average energy, temperature, and other measurable quantities were small (<5%).

## 3 Understanding the Relationship Between Surface Reactivity and Gold Atom Release

### 3.1 Release of Au Upon Adsorption of Electronegative Elements on Au(111): Effect on Surface Morphology

The interaction of electronegative atoms (specifically oxygen, chlorine, and sulfur) with gold is important to understand because of the number of applications in which they are used. Atomic oxygen is active for a wide range of oxidative transformations promoted by gold surfaces and nanoparticles [62–64]. Accordingly, most proposed mechanisms include atomic oxygen in at least one step of the catalytic cycle [89, 105–109]. Au–Cl interactions are of interest; for example, Au(III) chloride is used as a homogeneous catalyst for a number of important organic reactions including intramolecular cyclizations and cross-cycloisomerizations [110, 111]. Chlorine is used as a lixiviant for gold [112] and plays an important role in the contact between gold and semiconductor electrodes [113]. The interaction of sulfur and gold plays a vital role in the formation of self-assembled alkylthiol monolayers (SAMs) which have the possibility to be used in a wide variety of applications [114]. We are specifically interested in how the coverage of O, Cl, and S affects the morphology of the Au surface because experimental studies show that there are significant changes in both local bonding and overall morphology as a function of adsorbate coverage [115–117]. To this end, we have performed calculations that probe the interplay between the coverage of Cl and O and the energetics of defect formation.

Our results on Au(111) show that simple adsorption into an overlayer is most favorable for O and Cl on Au at low coverage, whereas Au adatom release becomes favorable at higher coverage. While Au(111) may be especially prone to the release of gold atoms due to the 'herringbone' reconstruction, which contains an excess of ~4.5% Au atoms compared to the bulk (111) plane [118–120], our theoretical and experimental results clearly show that gold

adatom release and bonding to, e.g. O, is also favored for the unreconstructed, close-packed (111) surface. Experimentally, we find that there are substantially more Au adatoms incorporated into the adsorbed layer, than the 4.5% excess in the herringbone reconstruction [115]. Scanning tunneling microscopy images in Fig. 1 illustrate this gold removal and also the dependence of the surface structure on oxygen coverage. Gold incorporation is even observed for molecular adsorption on the Au(111)-herringbone; for example, styrene [121], $NO_2$ [122], and $CH_3SH$ [123, 124] induce Au atom release.

In our theoretical calculations aimed at understanding the affect of atomic oxygen coverage on the morphology of gold [97], a $\left(\sqrt{3} \times \sqrt{3}\right)R30°$surface unit cell was used as a model for testing the energetics of gold incorporation versus overlayer coverage on Au(111) for oxygen coverages of 0.33, 0.66, and 1.00 ML. This model provides insight into coverage effects, but does not model the exact structure at higher coverage, which has a complex, disordered structure that is not amenable to study using periodic calculations. Therefore, factors, such as adsorbate–adsorbate repulsion that lead to Au incorporation, will only be qualitatively similar in the real and model systems, but the model will still provide insight into the coverage-dependent bonding of adsorbates on the gold surface.

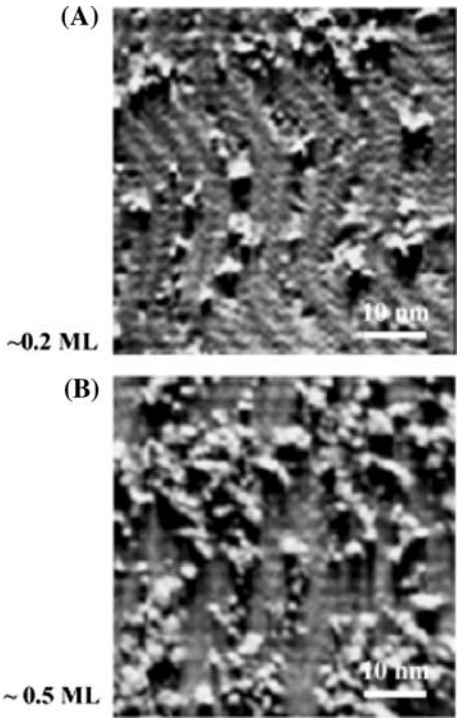


**Fig. 1** Scanning tunneling microscopic images (50 nm × 50 nm) of oxidized Au(111) surfaces where **a** 0.2 ML and **b** 0.5 ML of oxygen was deposited at 200 K using ozone. These images illustrate the roughening and restructuring of the gold surface upon adsorption of atomic oxygen. As the oxygen coverage increases, the number and size of islands increase and the 'herringbone' reconstruction is completely lifted (reprinted with permission from Ref. [62])

The approach we take to evaluating whether Au atom release is favored is to estimate the Gibbs free energy, $G(T, P, N_{Au}, N_O)$, using a technique described previously [125–127]. In this construction, the most stable surface minimizes the surface free energy, $\gamma(T, P)$, defined as:

$$\gamma(T,P) = (1/A)[G(T,P,N_{Au},N_O) - N_{Au}\mu_{Au}(T,P) - N_O\mu_O(T,P)]$$

where $\mu_{Au}$ and $\mu_O$ are the chemical potentials of a Au atom and an O atom, $N_{Au}$ and $N_O$ are the numbers of these species, and the surface energy has been normalized by dividing by the surface area, $A$ [125–127]. In principle the Gibbs free energy could be calculated by considering the contributions of vibrational and configurational entropy; in practice these contributions can be small and are often neglected allowing the terms to be approximated as DFT total energies [128]. Enthalpic contributions are likely the most prominent factor controlling the morphology of the surface, but it is important to note that entropic contributions can become important as discussed later in this report. The surface free energy becomes:

$$\gamma_{DFT}(T,P,n) = (1/A)[E_{Au/O} - E_{Au} - N_O\mu_O(T,P) + E_{cost}(n)]$$

Because the terms in the above expression can be related to DFT energies, this formula is very similar to the typical expression for the adsorption energy, where $E_{Au/O}$ is the total energy of the entire adsorbed system and $E_{Au}$ is the energy of the gold substrate. The last term, $E_{cost}$, has been added to account for the energetic cost for creating gold adatoms on the surface:

$$E_{cost}(n) = E_{s-ad}(n) - nE_b - E_s$$

with $E_{s\text{-}ad}(n)$ the total energy of the Au(111) substrate with $n$ adatoms, $E_b$ the energy of a gold atom in the bulk, and $E_s$, in this case, the energy of the bare Au(111) substrate. The chemical potential of oxygen could be related to an oxygen pressure and temperature by calculating the translational and rotational partition functions of the gas phase, but for a qualitative phase diagram it suffices to consider a range of chemical potentials [125]. Figure 2 is a plot of the surface free energy as a function of the oxygen chemical potential for the lowest energy structures for overlayer adsorption and gold incorporation. Oxygen dissociation is not thermodynamically favorable in the small unlabeled region in Fig. 2 at the lower bound of the chemical potential. As the oxygen chemical potential increases, a higher oxygen coverage is possible on the surface creating three distinct regions, labeled Ia, Ib, and II.

The structures with the lowest surface free energy in regions Ia and Ib are the 0.33 and 0.67 ML of oxygen coverage, respectively, both without gold adatom incorporation. Interestingly, a transition between flat overlayer adsorption and gold incorporation occurs between region I and II when the oxygen coverage with the lowest energy increases from 0.67 to 1.00 ML. At the higher oxygen coverage it is energetically favorable for gold atoms to be removed from the substrate and bind with oxygen atoms.

Our work agrees with Shi and Stampfl [129] who performed similar calculations using a larger unit cell; they predict, however, that the energetically most favorable configuration at all the coverages they tested, is a "surface-oxide-like" layer that has gold incorporated into its structure. Several other groups have also investigated oxygen adsorption on gold using DFT; however, the possibility of gold release from the surface induced by adsorbed O was not considered [31, 38, 89, 106, 130–132]. For example, Miller and Kitchin [130] calculated a surface free energy plot for different coverages and structures of oxygen on Au(111), but without considering structures involving Au extraction from the surface. Consideration of metal atom release is critical since changes in metal–metal bonding due to such added-metal structures will substantially affect bonding mechanisms and bond energies. In this regard, experiment plays a critical role in guiding theoretical studies, since atomic-scale imaging provides direct information about whether metal atom release must be considered or not. We also find, as described in the second section of this report, that gold incorporation significantly affects the reactivity of the surface for CO oxidation.

Both experiment (STM, see Fig. 3) and theory show a similar transition from overlayer adsorption at low coverage to gold incorporation at high coverage for Cl on Au(111) [97, 116]. Using DFT calculations, we have energetically verified experimental results using the same model $\left(\sqrt{3}\times\sqrt{3}\right)R30^{\circ}$ unit cell. To compare the adsorption of chlorine on each substrate (overlayer and gold incorporation structures), the total electronic energy is calculated in a similar fashion to the oxygen surface energy, which contains both the Cl binding energy and the cost for creating gold adatoms on the surface:

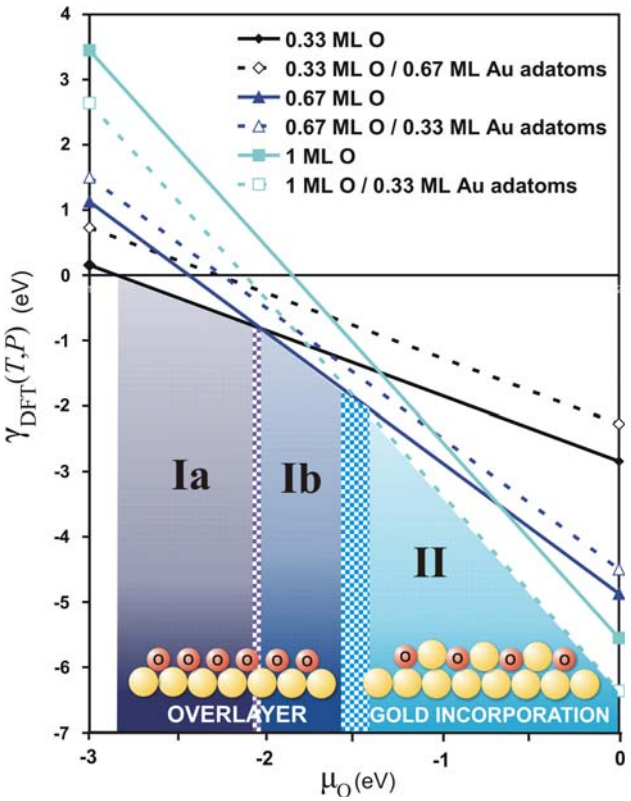


**Fig. 2** Surface free energy, $\gamma_{DFT}(T, P)$ as a function of the oxygen chemical potential, $\mu_O$ for different oxygen and gold adatom coverages. The clean surface is represented by a horizontal line at a surface free energy of 0 eV. The transition range in the oxygen chemical potential between regions, representing the error introduced by the choice of exchange-correlation functional, is indicated by checkered-square region (reprinted with permission from Ref. [97])

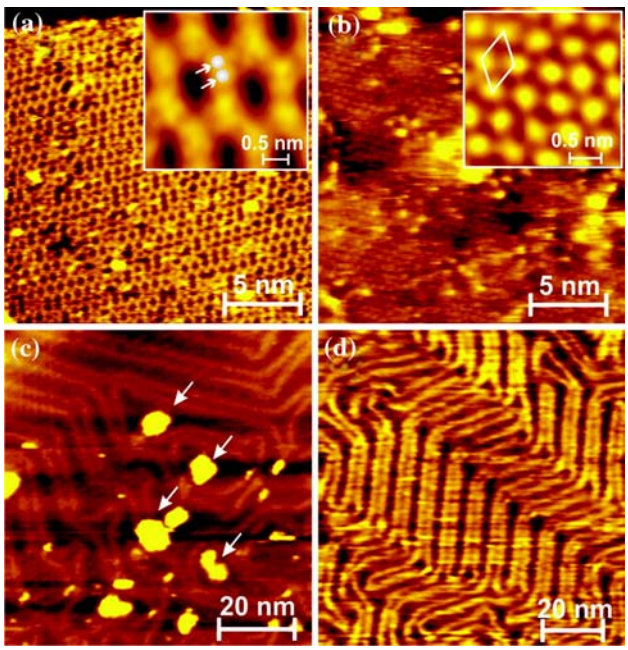


**Fig. 3** STM images of **a** ~0.8 ML chlorine on Au(111) showing the honeycomb structure. The inset shows that each unit in the hexagon adopts a dimer structure. **b** Flashing **a** to 750 K. **c** Annealing **a** at 750 K for 1 min. **d** Annealing **a** at 750 K for 5 min. $Cl_2$ is dosed at 300 K. All STM images were collected at 120 K. **a** Gold incorporation, which is verified in **c** where Cl has been removed by annealing but gold islands remain on the surface. However, when annealed for long enough the gold adatoms are incorporated back into the surface and the characteristic 'herringbone' reconstruction of Au(111) remains **d** (reprinted with permission from Ref. [116])

**Table 1** Summary of total electronic energies, $E_{total}(n,p)$, for two Cl coverages, $p$ (expressed in ML for the $(\sqrt{3} \times \sqrt{3})R30^\circ$ unit cell) on Au(111) with different gold adatom coverages, $n$

| $n$ (ML) | $p$ (ML) | | | |
|---|---|---|---|---|
| | 0.33 ML CI | | 0.67 ML CI | |
| | Site | $E_{total}$ (eV) | Site | $E_{total}$ (eV) |
| 0.00 | Top | −0.65 | Bridge | −0.37 |
| | Bridge | −0.87 | | |
| | HCP | −0.88 | | |
| | **FCC** | **−0.91** | | |
| 0.33 | Top | −0.43 | **$AuCl_2$** | **−0.54** |
| | Side | −0.47 | | |
| 0.67 | Bridge | −0.81 | **Half bridge** | **−0.57** |
| | Hollow | −0.24 | Top | −0.20 |

Bold characters indicate the systems with the lowest energy at each chlorine and adatom coverage (reprinted with permission from Ref. [116])

$$E_{total}(n,p) = E_{Cl-ads}(p) + E_{cost}(n)$$

where $E_{cost}(n)$ has been defined above and $E_{Cl\text{-}ads}(p)$ is the adsorption energy of Cl on the gold substrate defined as:

$$E_{Cl-ads}(p) = E_{Au/Cl} - E_s - \frac{p}{2}E_{Cl_2}$$

where $E_{Au/Cl}$ is the total energy of the system consisting of the Au surface with $p$ Cl atoms bound on the gold substrate, $E_s$ is the energy of the gold substrate, and $E_{Cl_2}$ is the energy of the $Cl_2$ molecule. A similar phase diagram could be produced for chlorine adsorption as was done for oxygen, but for simplicity only the $Cl_2$ binding energy is used; there is no change in the overall conclusions in doing so.

While there is a strong coverage dependence in the overall energetics for O and Cl adsorption on Au(111), there are differences in the two cases. In contrast to the oxygen results, the transition from overlayer adsorption to gold incorporation occurs between 0.33 and 0.67 ML of chlorine, compared to between 0.67 and 1.00 ML for O. Table 1 summarizes the calculated total energies for Cl. The chlorine structure with the lowest total energy is the overlayer with Cl in FCC three-fold sites, with a total energy of −0.91 eV, for a coverage of 0.33 ML. The configuration with 0.33 ML of gold adatoms has two chlorine atoms bound on top of a gold adatom on either side, coordinated only to the gold adatom. But at a higher coverage, 0.67 ML, the overlayer is no longer the lowest in energy; instead, the gold incorporated structures with 0.33 and 0.67 ML of gold adatoms are lowest in energy. The structure with 0.67 ML of chlorine adsorbed on 0.67 ML of gold adatoms (labeled 'half-bridge site' in Table 1) has Cl bound directly to one gold atom but in an off-center position, tilted towards the vacancy and close to what would have been the bridge site of the surface without the vacancy. An alternative structure, with the Cl atom directly on top of the gold atom is substantially higher in energy (Table 1). At both tested coverages of Cl, the Au–Cl interaction is stronger on the adatom covered surface, but when taking into account the cost of creating the adatom-covered surface, the 0.33 ML chlorine overlayer is lowest in energy while at 0.67 ML of chlorine, the adatom covered surfaces are lowest in energy. Other groups have performed important calculations of Cl on gold surfaces, but gold incorporation was not considered, which could have important implications on their results as discussed above for O [133–136]. However, Peljhan and Kokalj did allow metal incorporation for Cl adsorption on Cu(111) and they found many of the same trends [137].

Gold incorporation is also observed for sulfur adsorption on gold. Experiments revealed that sulfur adsorption at 300 K lifts the surface reconstruction of Au(111) in the low-coverage regime (0.1 ML) and leads to the formation of a 2D AuS phase involving large-scale mass transport in the high coverage regime (>0.3 ML). The reaction is completed once the S coverage reaches a value of approximately 0.6 ML. At this point, the surface is completely covered with an AuS overlayer, although it is broken into domains. Further annealing to 450 K decreases the sulfur coverage by approximately 20% (to 0.5 ML), and large vacancy islands of monatomic depth develop by Ostwald ripening of the original irregular etch pits. At this point, the Au(111) surface is uniformly covered (terrace areas as well as vacancy islands) with an ordered, incommensurate AuS film [117, 138].

Density functional theory has been used to develop an atomistic model of the AuS overlayer [139]. The structure obtained is robust, reflects the rich coordination chemistry of Au, and reproduces experimental observations. Since an incommensurate layer interacts only weakly with the substrate, first calculations were performed that considered an isolated AuS layer. Several models were explored with different numbers of atoms with the ratio Au:S = 1:1, which was found experimentally. Using a unit cell that was consistent with experiment, only one stable structure is found in which gold is incorporated, shown in Fig. 4. This layer is then placed on a Au(111) surface, the optimal configuration is found, and STM images were simulated in excellent agreement with the experimental results. A bonding analysis based on Wannier functions showed that the Au–S layer exhibits a rich coordination chemistry corresponding to different Au oxidation states.

It is clear from our work that electronegative atoms (like O, Cl, and S) incorporate gold into the adsorbate layer, even though the details of the structures and the coverages at which Au atom release is favored depends on the specific adsorbate. Past work has attributed adsorbate-induced

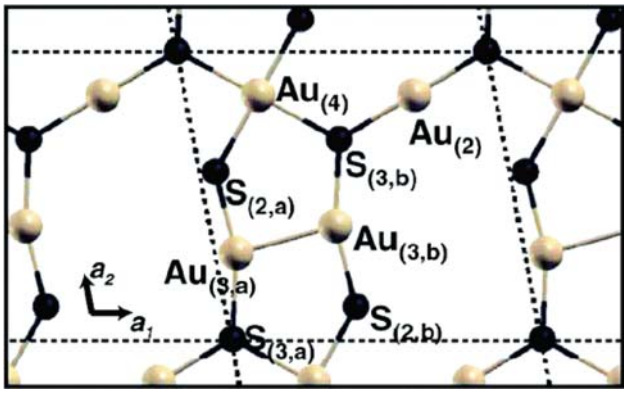


**Fig. 4** Model of planer Au–S layer. Light and dark spheres represent gold and sulfur, respectively. The numerical subscripts correspond to the coordination of each atom. The AuS structure is planar. The number and lower case letter in the parenthesis next to the labels of each atom indicate number of neighboring atoms and (when necessary) the distinction between two different atoms with the same coordination number (reprinted with permission from Ref. [139])

restructuring as thermodynamically driven to optimize the strength of the chemisorption bond. The exothermic heat of adsorption compensates for the relocation of metal atoms around the adsorption site that weakens metal–metal bonds [24].

We find two similar factors that contribute to gold incorporation: (1) the adsorbate-gold bond becomes stronger and changes (more covalent-like with a smaller amount of charge transfer) when gold is incorporated and (2) adsorbates can stabilize the presence of adatoms or other defects in the gold substrate. The first factor is not surprising since adsorption is often stronger with the presence of defects, and has been energetically verified for these systems in our previous calculations [96–98]. However, stronger adsorption does not ensure that the structure that incorporates Au is the lowest in energy since there is an energetic cost for creating under-coordinated gold atoms on the surface.

Electronic density plots reveal that adsorption on gold adatoms is generally more covalent in nature compared to overlayer adsorption, since bonding is more localized [97]. The stronger covalent interaction resulted in a smaller degree of charge transfer from the gold to the adsorbate, imparting a smaller partial negative charge compared to overlayer adsorption. This result provides an explanation for the dependence of gold incorporation on adsorbate coverage: as the coverage increases, the inter-adsorbate distance decreases and the Coulombic-repulsive interaction between the partially negatively charged adsorbates increases. Gold incorporation, however, decreases this negative charge since the adsorbate-gold bond becomes more covalent in nature. Hence, the repulsive interaction between adsorbates decreases.

Furthermore, analysis of our theoretical results using partial density of states (PDOS) plots show that electronegative adsorbates stabilize gold defects on the surface. A comparison of the Au *d*-PDOS for the Au(111)-(1 × 1) surface, the surface containing 0.33 ML of adatoms, and the adatom-covered surface with 0.67 ML Cl, provides insight into bonding changes (Fig. 5). As expected, without chlorine adsorbed on the surface, the Au *d* states are higher in energy for the gold adatoms, suggesting that adatoms are more reactive [79, 140]. With chlorine adsorbed, the gold adatom *d* electronic states are significantly lowered in energy, suggesting that adsorbed Cl can stabilize adatoms that are created on the surface. This helps explain why the adsorption energy for chlorine at any coverage is lower than the clean surface. Similar behavior is observed for other adsorbates suggesting this may be a general factor in explaining why metal atoms can be incorporated into the adsorbate structure.

### 3.2 Impact of Gold Release on Reactivity: AIMD Simulations of O Adsorption and CO Oxidation on Au(111)

The release of gold atoms not only affects the morphology of the surface as we have detailed in the previous section, but also changes the local bonding and the reactivity of oxygen. We specifically explored how gold incorporation affects the atomic oxygen species present for CO oxidation on Au(111). In the previous section, we used static DFT calculations to model the oxygen-covered gold surface; however, experiments show that this system is dynamic, disordered, and quite complex [115]. Unfortunately, modeling complex,

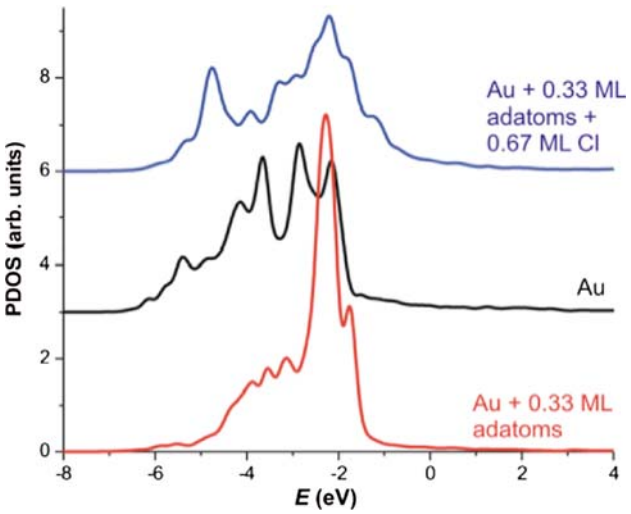


**Fig. 5** Au *d*-PDOS versus energy *E* for the surface gold atom of the clean surface (black), gold adatom for the 0.33 ML adatom-covered surface (red), and gold adatom for the 0.33 ML adatom-covered surface with 0.67 ML Cl (blue) (reprinted with permission from Ref. [97])

disordered systems presents a major challenge for theoretical treatment because a specific starting structure must be assumed. Indeed, previous theoretical studies of CO oxidation on Au surfaces have used static, zero-temperature DFT calculations [56, 89, 141–155].

A popular theoretical technique used for modeling dynamic events on surfaces is kinetic Monte Carlo (kMC) [156], but it presumes prior complete knowledge of events important to the dynamics of the system. Furthermore, the spatial degrees of freedom of the system are typically reduced to a simple lattice. For the complicated dynamical interaction of oxygen with gold it is impossible to know all the important events a priori and it is unrealistic to confine these events within the context of a lattice. Ideally, a fully-atomistic molecular dynamics simulation with accurate forces between ions and under realistic external conditions (temperature and oxygen concentration) would be used to capture all relevant effects.

Recently, we developed the ability to use ab initio molecular dynamics (AIMD) simulations to model the dynamic restructuring of the Au(111) surface due to the adsorption of atomic oxygen. We simulated the adsorption of atomic oxygen at three different coverages (0.22, 0.33, and 0.55 ML) and three different temperatures (200, 500, 800 K) using AIMD. We found that the morphology and local binding site of oxygen depends on the coverage and the surface temperature, in agreement with experimental results. Calculated vibrational frequencies derived from these simulations are in agreement with vibrational spectroscopy experiments [157].

Three different categories of O on the surface were identified in our simulations: (1) chemisorbed oxygen bound to a threefold hollow site, similar to that identified at low coverage in our static DFT studies; (2) surface oxide, which incorporates gold into the structure; and (3) subsurface oxide, in which O migrates to the subsurface region, Fig. 6. At low oxygen coverage (<0.33 ML) or temperature (200 K), the Au(111) surface is smooth and contains mostly the overlayer of chemisorbed oxygen, in agreement with our static DFT calculations. At higher coverages (>0.33 ML) or temperatures (500, 800 K), the surface forms a significant amount of surface and subsurface oxide species, defined above. Experimental measurements of vibrational spectra also show that the local bonding of O depends on the coverage and on the surface temperature [157], with the chemisorbed O favored at low coverage and low surface temperature (200 K).

Based on experiment, the reactivity of O also depends on local bonding. For example, the rate of CO oxidation is faster for the predominant species at low coverage and low temperature [62]. By matching calculated vibrational spectra with the experimental results under conditions that produce the most reactive surface for CO and olefin oxidation, our AIMD simulations suggested that chemisorbed oxygen, i.e. O in local threefold hollow sites, was the most reactive species for CO oxidation on Au(111).

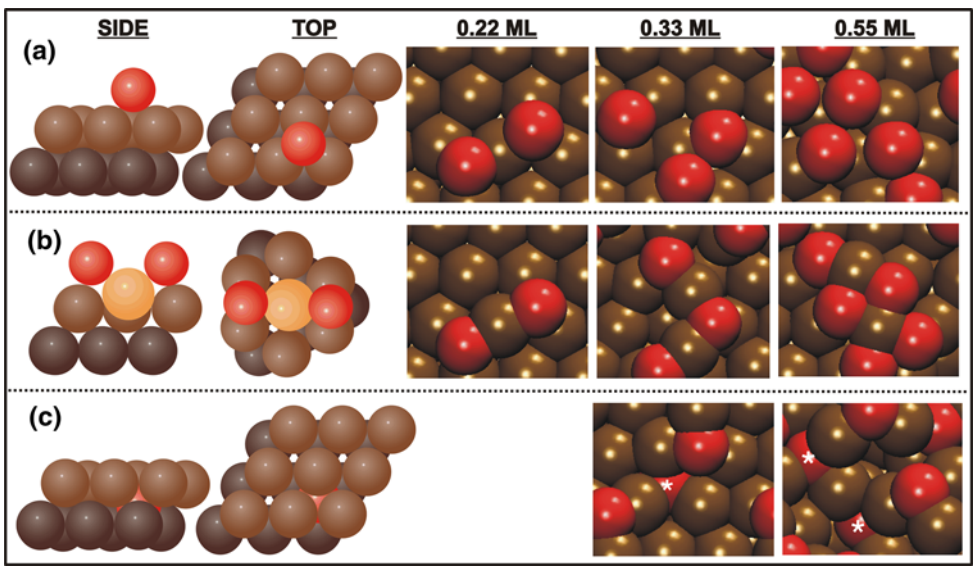


**Fig. 6** Model (*left*) and examples (*right*) of the three oxygen species: **a** chemisorbed, **b** surface oxide, and **c** subsurface oxide. A prototypical model of each oxygen type is shown on the left. Dark brown, light brown, yellow, and red spheres represent the second layer of gold, top layer of gold, gold adatoms, and oxygen atoms, respectively. Illustrative examples of each oxygen type at each coverage are shown on the right. Brown and red spheres represent gold and oxygen atoms, respectively. An asterisk labels subsurface oxygen atoms in **c**. We did not observe the subsurface oxide below an oxygen coverage of 0.33 ML

To test this hypothesis, we simulated the oxidation of CO on oxygen-covered Au(111) surface using AIMD to model the dynamics of the reaction, and confirmed our predictions regarding the nature of the reactive oxygen. The adsorption of CO and its oxidation to $CO_2$ on an oxygen-covered Au(111) surface at 500 K was simulated at three different oxygen coverages: 0.22, 0.33, and 0.55 ML [99]. We observed varying degrees of adsorption and reactivity as a function of the coverage. Compared to adsorption on the oxygen-free surface, CO has a longer average residence time on the surface, however, the adsorption lifetime decreases with increasing oxygen coverage. Earlier theoretical [157] and experimental [115] work has shown that with increasing oxygen coverage, the gold surface becomes rough and consists of a higher concentration of under-coordinated surface gold atoms. It has been suggested in a variety of systems, including supported Au nanoparticles [56, 131, 155, 158, 159] and Au clusters on Au(111) [90, 108], that under-coordinated surface gold atoms are the key factor to gold activity and the increased residence time could be a cause of this effect.

Reactions involving a chemisorbed oxygen atom proceed mainly through one pathway, labeled $A_1$ in Fig. 7. In this pathway a CO molecule is bound on top of a gold atom neighboring a three-fold site. During the reaction, the CO molecule moves into the bridge site and towards the oxygen, while at the same time the O atom moves towards the CO through the same two-fold site. The C of the CO molecule meets the absorbed oxygen atom forming $CO_2$ which then desorbs from the surface. A less frequent pathway for CO reaction with chemisorbed oxygen, labeled $A_2$ in Fig. 7, occurs when CO binds to the same gold atom to which an adsorbed oxygen is bound to in a three-fold site. The reaction following adsorption is fast due to the instability of the system and because the CO molecule can easily find the adsorbed oxygen atom. Other reactions involving a gold adatom occur when the carbon reacts with chemisorbed oxygen ($E_1$) or the surface oxide or sub-surface oxygen ($E_2$). Carbon monoxide oxidation was previously studied in several static DFT calculations; Su et al. [141] found a barrier of 0.29 eV for the oxidation on the Au(111) surface, while Liu et al. [89] found a barrier of 0.25 eV for the same reaction on the Au(221) surface. The careful work of Wang et al. also showed that the barrier and rate of CO oxidation depends the coordination of gold atoms using static DFT [90].

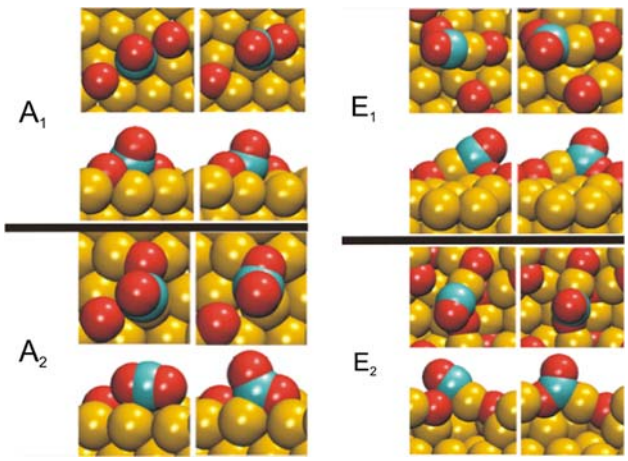


**Fig. 7** Snapshots (top and side views) of reaction pathways for CO oxidation to $CO_2$ on oxygen covered Au(111) surfaces. Yellow, blue, and red spheres represent gold, carbon, and oxygen atoms, respectively. Reaction $E_1$ and $E_2$ differ in that CO reacts with a chemisorbed oxygen in the former, while CO reacts with a surface oxide in the latter. The first column illustrates the start of the reaction while the second column approximates the transition state

We find the most reactive surface to be the one with 0.22 ML of oxygen, in mostly chemisorbed form. Table 2 breaks down the oxygen type present at 0.22 and 0.33 ML of oxygen and the oxygen type that participates in the reaction at each coverage. The type of oxygen present before reaction is also determined from separate AIMD calculations and the oxygen type that participates in each reaction is found by analyzing each independent AIMD trajectory that resulted in CO oxidation. The chemisorbed oxygen contributes to the majority of the oxidation reactions. For 0.22 ML of oxygen coverage, initially 80% of the surface is covered with chemisorbed oxygen while 20% is covered in surface oxide. However, of the oxygen type responsible for oxidation, 86% is chemisorbed oxygen. The same is true for 0.33 ML of oxygen: the surface is covered with 60% of chemisorbed oxygen, yet chemisorbed oxygen makes up 83% of the reactive atoms, illustrating that the chemisorbed oxygen is the most reactive type on the surface. Table 2 also illustrates the calculated relative reaction rate for each oxygen type. Even when the rate is normalized to take into account the ratio of each oxygen species on the surface (bottom line of Table 2), the relative rate for reaction with chemisorbed oxygen (overlayer) is significantly higher than surface oxide (gold incorporation). This work illustrates the effect on reactivity due to the surface morphology.

### 3.3 Future Challenges

We have demonstrated the value of using DFT-based dynamical simulations to model disordered systems. Unfortunately, these methods require substantial computational resources and for the systems we are interested in, they are limited to short simulation times, $\sim$10 ps. Generally, two key factors need to be taken into consideration when simulating such systems: the ability to accurately describe the important characteristics of the system (such as the forces between nuclei, charge transfer, etc.) and the

**Table 2** Ratio of chemisorbed oxygen and surface oxide on the surface before CO oxidation (surface species) and the oxygen atom type consumed during oxidation (reactive species) along with the relative rate and normalized relative rate (by oxygen type) for the reaction for each oxygen type on 0.22 and 0.33 ML oxygen covered Au(111)

| | 0.22 ML | | 0.33 ML | |
|---|---|---|---|---|
| | Chemisorbed | Surface oxide | Chemisorbed | Surface oxide |
| Surface species | 0.80 | 0.20 | 0.60 | 0.40 |
| Reactive species | 0.88 | 0.12 | 0.83 | 0.17 |
| Relative rate | 7.7 | 1.0 | 5.0 | 1.0 |
| Normalized relative rate | 1.9 | 1.0 | 3.3 | 1.0 |

need to minimize the computational cost of the simulation so that the dynamics of the system can be modeled for long time scales. Coarse-grained and lattice based methods, such as kMC, are capable of investigating processes over a long time scale but these methods must simplify the complicated electronic and ionic system using approximations, or reduce the dimensionality of the fully atomistic system to a lattice. For systems as complicated as the interaction of adsorbates on gold, neither of these approximations is acceptable. To avoid this problem, fully atomistic simulations can be done with forces between nuclei accurately calculated using DFT, but this level of accuracy is computationally costly resulting in short dynamical runs. Future calculations where the computational cost can be kept to a minimum will undoubtedly be performed using ab initio molecular dynamics or other accurate dynamical methods (for example, Car-Parrinello molecular dynamics) to understand the reactivity of catalytic surfaces.

Along with dynamic methods, static density functional theory calculations have provided valuable insight into surface phenomenon. These calculations will most likely become more important in catalysis as they improve and develop. Their increased use, however, depends on solving some very important problems in using theory to understand catalysis. While modern DFT can provide accurate results for many properties of a material (for example, the GGA exchange-correlation functional can provide accurate lattice constants and bond distances for a wide range of metals and other solids [160]), other simple properties, like adsorption energies, can have significant errors for many systems important in catalysis. The development of better exchange-correlation functionals along with other novel methods is vital to improve the accuracy and applicability of DFT calculations. The speed of the calculations is also another important concern; the capability to simulate larger systems allows for larger unit cells and the ability to model a wider range of systems. While theorists will gain some 'free' speed as computer hardware improves, more work is needed to improve the efficiency of simulations along with the scaling of computational cost versus simulation size.

When calculating reaction rates and barriers another important but often overlooked factor is the contribution of entropy to the free energy. Changes in entropy (or the entropy of activation) can be approximated using DFT by calculating the partition function, which can be found within the harmonic approximation by calculating vibrational frequencies [128, 161]. However, accurate vibrational frequencies can be computationally expensive and different approximations (for example, the choice of atoms within the system to freeze) can produce different energies. Furthermore, the temperature dependence of enthalpy is often not considered. The entropic contributions in some catalytic systems may be small enough (<0.1 eV) to be neglected [128], but there are likely systems where entropic contributions and zero-point energy corrections can have a significant contribution. For example, Valdes et al. found these contributions to be $\sim$0.4 eV for reactions important for the oxidation and photo-oxidation of water on rutile $TiO_2$(110) [162]. Future work will include efficient and accurate methods for calculating the change in entropy during reactions.

Finally, theoretical tools are needed to model a wider range of phenomenon, which can allow for a better match with experimental observations. Progress will need to continue if we hope to use DFT to simulate the interaction of photons and electrons with solids (for calculating different types of vibrational and electronic spectra), improve the ability of DFT to simulate STM images, reactions and kinetic properties, and other important properties which can improve the range of insight found from DFT along with providing more connections to experimental observations.

## 4 Conclusions and Relationship to Modeling of Heterogeneous Catalysis

Metal atom incorporation upon adsorption is an important factor to consider when understanding the chemistry and physics of metal surfaces as shown in both our experimental and theoretical work. The investigation of Au atom release and incorporation induced by electronegative atoms

clearly illustrates the importance of using experimental results to inform the theoretical model, which leads to an understanding of the underlying reasons for specific chemical behavior.

In our theoretical work to date, we have demonstrated that Au atom release significantly affects the surface morphology, local bonding, and reactivity of adsorbed species, especially for the interaction of electronegative atoms on Au(111). Overlayer adsorption without metal atom release is energetically preferred at lower coverages while gold incorporation is favored at higher coverages.

In an effort to probe for differences in the reactivity of different types of adsorbed O, dynamical ab initio molecular dynamics simulations were used to simulate CO oxidation on oxygen covered Au(111). We found that chemisorbed oxygen in three-fold sites is significantly more reactive than gold incorporated structures (surface oxide and sub-surface oxygen). These results suggest that Au activity will be highest for lower temperature and low coverages, in agreement with experiment.

Our results are a basis for including metal atom release in realistic simulations of catalytic reactions on surfaces. It is clear from our work that gold incorporation must be included in static theoretical models that are used to understand either adsorption or reactions on gold surfaces, especially at high coverage. The absence of metal atom release at low coverage, at least when O and Cl are adsorbed on Au(111), suggests that metal atom release is not as favorable in the low coverage limit. It is interesting to note that calculations that do not account for metal release have demonstrated predictive value for heterogeneous catalysis [76], which may be due to the fact that most catalytic processes are designed to operate under conditions where steady state coverages of reactants are low.

## References


1. Asscher M, Somorjai GA (1984) Surf Sci 143:L389
2. Strongin DR, Bare SR, Somorjai GA (1987) J Catal 103:289
3. Ertl G (1991) In: Jennings JR (ed) Elementary steps in ammonia synthesis: the surface science approach in catalytic ammonia synthesis. Springer, New York
4. Somorjai GA (1999) Introduction to surface chemistry and catalysis. Wiley–VCH, New York
5. Thiel PA, Estrup PJ (1995) In: Hubbard AT (ed) Surface metal reconstructions in CRC handbook of surface imaging and visualization. CRC Press, Boca Raton, FL, p 407
6. Somorjai GA (1995) Prog Surf Sci 50:3
7. Ertl G (2001) Chem Rec 1:33
8. Norskov JK, Bligaard T, Hvolbaek B, Abild-Pedersen F, Chorkendorff I, Christensen CH (2008) Chem Soc Rev 37:2163
9. Guo XC, Madix RJ (2003) Accounts Chem Res 36:471
10. Starke U, Vanhove MA, Somorjai GA (1994) Prog Surf Sci 46:305
11. Vanhove MA, Somorjai GA (1994) Surf Sci 299:487
12. Marsh AL, Somorjai GA (2005) Top Catal 34:121
13. Somorjai GA, Hwang KS, Parker JS (2003) Top Catal 26:87
14. Devarajan SP, Hinojosa JA, Weaver JF (2008) Surf Sci 602:3116
15. Hawkins JM, Weaver JF, Asthagiri A (2009) Phys Rev B 79:13
16. Helveg S, Lorensen HT, Horch S, Laegsgaard E, Stensgaard I, Jacobsen KW, Norskow JK, Besenbacher F (1999) Surf Sci 430:L533
17. Li WX, Osterlund L, Vestergaard EK, Vang RT, Matthiesen J, Pedersen TM, Laegsgaard E, Hammer B, Besenbacher F (2004) Phys Rev Lett 93:4
18. Kan HH, Weaver JF (2008) Surf Sci 602:L53
19. Niehus H, Comsa G (1985) Surf Sci 151:L171
20. Kleinle G, Wintterlin J, Ertl G, Behm RJ, Jona F, Moritz W (1990) Surf Sci 225:171
21. Yarmoff JA, Cyr DM, Huang JH, Kim S, Williams RS (1986) Phys Rev B 33:3856
22. Jensen F, Besenbacher F, Stensgaard I (1992) Surf Sci 259:L774
23. Sokolov J, Jona F, Marcus PM (1986) Europhys Lett 1:401
24. Somorjai GA, Borodko Y (1999) Catal Lett 59:89
25. Tao F, Dag S, Wang LW, Liu Z, Butcher DR, Salmeron M, Somorjai GA (2009) Nano Lett 9:2167
26. Mase K, Yoshitada M (1992) Surf Sci 277:97
27. Norton PR, Griffiths K, Binder PE (1984) Surf Sci 138:125
28. McCrea K, Parker JS, Chen P, Somorjai GA (2001) Surf Sci 494:238
29. Zhou L, Gao WW, Klust A, Madix RJ (2008) J Chem Phys 128:6
30. Haruta M, Date M (2001) Appl Catal A-Gen 222:427
31. Haruta M (2003) Chem Rec 3:75
32. Meyer R, Lemire C, Shaikhutdinov SK, Freund H (2004) Gold Bull 37:72
33. Schwank J (1983) Gold Bull 16:103
34. Kolasinski KW (2008) Surface science: foundations of catalysis and nanoscience. Wiley, New York
35. Lee DW, Ryu JH, Jeong DH, Lee HS, Chun KM, Lee KY (2003) J Ind Eng Chem 9:102
36. Jang BWL, Spivey JJ, Kung MC, Kung HH (1997) Energy Fuels 11:299
37. Grisel RJH, Kooyman PJ, Nieuwenhuys BE (2000) J Catal 191:430
38. Grisel RJH, Neiuwenhuys BE (2001) Catal Today 64:69
39. Haruta M, Yamada N, Kobayashi T, Iijima S (1989) J Catal 115:301
40. Hayashi T, Tanaka K, Haruta M (1998) J Catal 178:566
41. Stangland EE, Stavens KB, Andres RP, Delgass WN (2000) J Catal 191:332
42. Laibinis PE, Whitesides GM, Allara DL, Tao Y, Parikh AN, Nuzzo RG (1991) J Am Chem Soc 113:7152
43. Ulman A (1996) Chem Rev 96:1533
44. Kumar A, Biebuyck HA, Whitesides GM (1994) Langmuir 10:1498
45. Fischer CM, Burghard M, Rith S, Klitzing KV (1995) Appl Phys Lett 66:3331
46. Ellis AV, Vijayamohanan K, Goswami R, Chakrapani N, Ramanathan LS, Ajayan PM, Ramanath G (2003) Nano Lett 3:279
47. Ozturk B, Blackledge C, Flanders BN, Grischkowsky DR (2006) Appl Phys Lett 88:073108
48. Janata J, Josowicz M (2003) Nat Mater 2:19
49. Liu J, Lu Y (2003) J Am Chem Soc 125:6642
50. Siwy Z, Trofin L, Kohli P, Baker LA, Trautmann C, Martin CR (2005) J Am Chem Soc 127:5000
51. Ozbay E (2006) Science 311:189
52. Biener J, Nyce GW, Hodge AM, Biener MM, Hamza AV, Maier SA (2008) Adv Mater 20:1211

53. Valden M, Pak S, Lai X, Goodman DW (1998) Catal Lett 56:7
54. Valden M, Lai X, Goodman DW (1998) Science 281:1647
55. Comotti M, Li WC, Spliethoff B, Schuth F (2006) J Am Chem Soc 128:917
56. Lopez N, Janssens TVW, Clausen BS, Xu Y, Mavrikakis M, Bligaard T, Norskov JK (2004) J Catal 223:232
57. Zhu BL, Angelici RJ (2006) J Am Chem Soc 128:14460
58. Iizuka Y, Tode T, Takao T, Yatsu K, Takeuchi T, Tsubota S, Haruta M (1999) J Catal 187:50
59. Zielasek V, Jurgens B, Schulz C, Biener J, Biener MM, Hamza AV, Baumer M (2006) Angew Chem Int Ed 45:8241
60. Xu CX, Su JX, Xu XH, Liu PP, Zhao HJ, Tian F, Ding Y (2007) J Am Chem Soc 129:42
61. Yin H, Zhou C, Xu C, Liu P, Xu X, Ding Y (2008) J Phys Chem C 112:9673
62. Min BK, Alemozafar AR, Pinnaduwage D, Deng X, Friend CM (2006) J Phys Chem B 110:19833
63. Deng XY, Min BK, Liu XY, Friend CM (2006) J Phys Chem B 110:15982
64. Deng XY, Friend CM (2005) J Am Chem Soc 127:17178
65. Liu XY, Madix RJ, Friend CM (2008) Chem Soc Rev 37:2243
66. Min BK, Friend CM (2007) Chem Rev 107:2709
67. Min BK, Deng XY, Liu XY, Friend CM, Alemozafar AR (2009) ChemCatChem 1:116
68. Xu W, Kong JS, Yeh YE, Chen P (2008) Nat Mater 7:992
69. Falsig H, Hvolbaek B, Kristensen IS, Jiang T, Bligaard T, Christensen CH, Norskov JK (2008) Angew Chem Int Ed 47: 4835
70. Hvolbaek B, Janssens TVW, Clausen BS, Falsig H, Christensen CH, Norskov JK (2007) Nano Today 2:14
71. Janssens TVW, Clausen BS, Hvolbaek B, Falsig H, Christensen CH, Bligaard T, Norskov JK (2007) Top Catal 44:15
72. Remediakis IN, Lopez N, Norskov JK (2005) Appl Catal A-Gen 291:13
73. Lemire C, Meyer R, Shaikhutdinov SK, Freund HJ (2004) Surf Sci 552:27
74. Janssens TVW, Carlsson A, Puig-Molina A, Clausen BS (2006) J Catal 240:108
75. Schubert MM, Plzak V, Garche J, Behm RJ (2001) Catal Lett 76:143
76. Norskov JK, Bligaard T, Rossmeisl J, Christensen CH (2009) Nat Chem 1:37
77. Somorjai GA, Kliewer CJ (2009) React Kinet Catal Lett 96:191
78. Christensen CH, Norskov JK (2008) J Chem Phys 128:8
79. Hammer B, Norskov JK (2000) Adv Catal 45:71
80. Hellman A, Honkala K, Remediakis IN, Logadottir A, Carlsson A, Dahl S, Christensen CH, Norskov JK (2009) Surf Sci 603:1731
81. Greeley J, Norskov JK (2009) J Phys Chem C 113:4932
82. Jones G, Jakobsen JG, Shim SS, Kleis J, Andersson MP, Rossmeisl J, Abild-Pedersen F, Bligaard T, Helveg S, Hinnemann B, Rostrup-Nielsen JR, Chorkendorff I, Sehested J, Norskov JK (2008) J Catal 259:147
83. Nørskov JK, Bligaard T, Logadottir A, Bahn S, Hansen LB, Bollinger M, Bengaard H, Hammer B, Sljivcancanin Z, Mavrikakis M, Xu Y, Dahl S, Jacobsen JH (2002) J Catal 209: 275
84. Bligaard T, Norskov JK, Dahl S, Matthiesen J, Christensen CH, Sehested J (2004) J Catal 224:206
85. Michaelides A, Liu ZP, Zhang CJ, Alavi A, King DA, Hu P (2003) J Am Chem Soc 125:3704
86. Cheng J, Hu P (2008) J Am Chem Soc 130:10868
87. Hammer B, Norskov JK (1995) Nature 376:238
88. Mavrikakis M, Hammer B, Norskov JK (1998) Phys Rev Lett 81:2819
89. Liu ZP, Hu P, Alavi A (2002) J Am Chem Soc 124:14770
90. Wang HF, Gong XQ, Guo YL, Guo Y, Lu G, Hu P (2009) J Phys Chem 113:6124
91. Honkala K, Hellman A, Remediakis IN, Logadottir A, Carlsson A, Dahl S, Christensen CH, Norskov JK (2005) Science 307:555
92. Abild-Pedersen F, Greeley J, Norskov JK (2005) Catal Lett 105:9
93. Abild-Pedersen F, Lytken O, Engbaek J, Nielsen G, Chorkendorff I, Norskov JK (2005) Surf Sci 590:127
94. Ciobica IM, van Santen RA (2003) J Phys Chem B 107:3808
95. Jiang T, Mowbray DJ, Dobrin S, Falsig H, Hvolbaek B, Bligaard T, Norskov JK (2009) J Phy Chem C 113:10548
96. Baker TA, Friend CM, Kaxiras E (2009) J Phys Chem C 113:3232
97. Baker TA, Friend CM, Kaxiras E (2009) J Chem Phys 130: 084701
98. Baker TA, Friend CM, Kaxiras E (2008) J Chem Phys 129:5
99. Baker TA, Friend CM, Kaxiras E (2009) J Chem Theory Comput 6:279
100. Kresse G, Hafner J (1993) Phys Rev B 47:558
101. Vanderbilt D (1990) Phys Rev B 41:7892
102. Kresse G, Hafner J (1994) J Phys-Condes Matter 6:8245
103. Perdew JP, Wang Y (1992) Phys Rev B 45:13244
104. Nose S (2002) Mol Phys 100:191
105. Outka DA, Madix RJ (1987) Surf Sci 179:351
106. Xu Y, Mavrikakis M (2003) J Phys Chem B 107:9298
107. Yoon B, Hakkinen H, Landman U (2003) J Phys Chem A 107:4066
108. Mills G, Gordon MS, Metiu H (2003) J Chem Phys 118:4198
109. Stiehl JD, Kim TS, McClure SM, Mullins CB (2004) J Am Chem Soc 126:13574
110. Hashmi ASK, Schwarz L, Choi JH, Frost TM (2000) Angew Chem Int Ed 39:2285
111. Stephen A, Hashmi K, Frost TM, Bats JW (2000) J Am Chem Soc 122:11553
112. Nesbitt CC, Milosavljevic EB, Hendrix JL (1990) Ind Eng Chem Res 29:1696
113. Williams RH, Montgomery V, Varma RR, McKinley A (1977) J Phys D Appl Phys 10:L253
114. Love JC, Estroff LA, Kriebel JK, Nuzzo RG, Whitesides GM (2005) Chem Rev 105:1103
115. Min BK, Deng X, Pinnaduwage D, Schalek R, Friend CM (2005) Phys Rev B 72:4
116. Gao WW, Baker TA, Zhou L, Pinnaduwage DS, Kaxiras E, Friend CM (2008) J Am Chem Soc 130:3560
117. Biener MM, Biener J, Friend CM (2005) Langmuir 21:1668
118. Narasimhan S, Vanderbilt D (1992) Phys Rev Lett 69:1564
119. Bach CE, Giesen M, Ibach H, Einstein TL (1997) Phys Rev Lett 78:4225
120. Ibach HJ (1994) Vac Sci Technol A-Vac Surf Films 12:2240
121. Baber AE, Jensen SC, Iski EV, Sykes CH (2006) J Am Chem Soc 128:15384
122. Driver SM, Zhang TF, King DA (2007) Angew Chem Int Ed 46:700
123. Maksymovych P, Sorescu DC, Dougherty D, Yates JT (2005) J Phys Chem B 109:22463
124. Molina LM, Hammer B (2002) Chem Phys Lett 360:264
125. Kaxiras E, Baryam Y, Joannopoulos JD, Pandey KC (1987) Phys Rev B 35:9625
126. Qian GX, Martin RM, Chadi DJ (1988) Phys Rev B 38:7649
127. Reuter K, Scheffler M (2003) Phys Rev B 68:045407
128. Reuter K, Scheffler M (2001) Phys Rev B 65:035406
129. Shi H, Stampfl C (2007) Phys Rev B 76:075327
130. Miller SD, Kitchin JR (2009) Surf Sci 603:794
131. Mavrikakis M, Stoltze P, Morskov JK (2000) Catal Lett 64:101
132. Torres D, Neyman KM, Illas F (2006) Chem Phys Lett 429:86
133. Lemoine D, Quattrucci JG, Jackson B (2002) Phys Rev Lett 89:4

134. Migani A, Sousa C, Illas F (2005) Surf Sci 574:297
135. Quattrucci JG, Jackson B, Lemoine D (2003) J Chem Phys 118:2357
136. Migani A, Illas F (2006) J Phys Chem B 110:11894
137. Peljhan S, Kokalj A (2009) J Phys Chem C 113:14363
138. Min BK, Alemozafar AR, Biener MM, Biener J, Friend CM (2005) Top Catal 36:77
139. Quek SY, Biener MM, Biener J, Bhattacharjee J, Friend CM, Waghmare UV, Kaxiras E (2006) J Phys Chem B 110:15663
140. Hoffmann R (1988) Rev Mod Phys 60:601
141. Su HY, Yang MM, Bao XH, Li WX (2008) J Phys Chem C 112:17303
142. Broqvist P, Molina LM, Gronbeck H, Hammer B (2004) J Catal 227:217
143. Coquet R, Howard KL, Willock DJ (2008) Chem Soc Rev 37:2046
144. Prestianni A, Martorana A, Ciofini I, Labat F, Adamo C (2008) J Phys Chem C 112:18061
145. Fajin JLC, Cordeiro M, Gomes JRB (2008) J Phys Chem C 112:17291
146. Chen Y, Crawford P, Hu P (2007) Catal Lett 119:21
147. Wang CM, Fan KN, Liu ZP (2007) J Am Chem Soc 129:2642
148. Ganesh R, Pala S, Liu F (2006) J Chem Phys 125:5
149. Zhang CJ, Hu P (2000) J Am Chem Soc 122:2134
150. Molina LM, Lesarri A, Alonso JA (2009) Chem Phys Lett 468:201
151. Liu LM, McAllister B, Yu HQ, Hu P (2006) J Am Chem Soc 128:4017
152. Liu ZP, Jenkins SJ, King DA (2004) Phys Rev Lett 93:156102
153. Liu ZP, Gong XQ, Kohanoff J, Sanchez C, Hu P (2003) Phys Rev Lett 91:266102
154. Kandoi S, Gokhale AA, Grabow LC, Dumesic JA, Mavrikakis M (2003) Catal Lett 93:93
155. Remediakis IN, Lopez N, Norskov JK (2005) Angew Chem Int Ed 44:1824
156. Battaile CC, Srolovitz DJ (2002) Annu Rev Mater Res 32:297
157. Baker TA, Xu BJ, Liu XY, Kaxiras E, Friend CM (2009) J Phys Chem C 113:16561
158. Lopez N, Norskov JK (2002) J Am Chem Soc 124:11262
159. Lemire C, Meyer R, Shaikhutdinov S, Freund HJ (2004) Angew Chem Int Ed 43:118
160. Kohanoff J (2006) Electronic structure calculations for solids and molecules: theory and computational methods. Cambridge University Press, Cambridge
161. Ashcroft NW, Mermin ND (1981) Solid state physics. CBS Publishing, Tokyo
162. Valdes A, Qu ZW, Kroes GJ, Rossmeisl J, Norskov JK (2008) J Phys Chem C 112:9872